Landslides (2019) 16:1243–1251
DOI 10.1007/s10346-019-01135-5
Received: 22 October 2018
Accepted: 4 January 2019
Published online: 28 January 2019

Jiren Xie · Taro Uchimura · Pan Chen · Jiapeng Liu · Canrong Xie · Quan Shen

A relationship between displacement and tilting angle of the slope surface in shallow landslides

Abstract Tilt sensors with low cost and simple installation were developed for slope monitoring, but there is limited evidence to testify that the tilting angle of slope surface can be considered as an important indication of landslides, similar as the displacement of slope surface. In this study, the relationship between displacement and tilting angle of the slope surface in shallow landslides was investigated by the laboratory tests under different testing condition and field tests in which the slope failure was induced by applying artificial rainfall. A linear relationship between the displacement and tilting angle of slope surface was detected, and the equation for this linear relationship was also proposed in this study. Furthermore, the results also indicated that the linear relationship between the displacement and tilting angle of slope surface is independent of triggering factors of slope failure, materials of slopes, as well as the slopes sizes.

Keywords Landslides · Tilting angle · Displacement · Relationship

Introduction

Landslides which are mainly caused by heavy rainfall and strong earthquakes, are the major threat to human lives and property (Petley 2012; Keefer et al. 1987). To prevent the landslide disaster, typical countermeasures, such as retaining walls and ground anchors, have been widely used to improve the factor of safety against slope failure. However, those methods are not suitable for a large number of slopes with potential risks of slope failure due to the high cost (Uchimura et al. 2015).

Developing an early warning system is a promising way to assess the risks of landslides and minimize losses caused by landslides. In past decades, some early warning systems have been proposed to measure the displacement of slope surface using extensometers and employed in many cases of slope monitoring (Saito 1987; Emanuele 2012; Fukuzono 1985). For those early warning systems, skilled and experienced engineerers are required to install the instruments and maintain the systems, which increase the cost and limit the application of those systems.

Some studies show that the tilting behavior of slope surface could be treated as an indication of landslides considering that tilting angle of slopes raises with the increase of displacement based on results of model tests (Iverson et al. 2000). In recent years, with the development of microelectronic techniques, new low-cost real-time monitoring systems using MEMS (Micro Electro Mechanical Systems) technology have been developed to detect the pre-failure tilting behavior in shallow landslides (Towhata et al. 2005; Uchimura et al. 2008, 2010, 2015). In these new developed systems, the tilting behavior of slopes was measured by tilt sensors together with steel rods which were vertically installed in the slope surface as shown in Fig. 1. Although the tilt sensors in these systems are less costly and easier to be installed than extensometers, limited studies were carried out to verify that tilt sensors can take the place of extensometers in slope monitoring for shallow landslide.

The main aim of this paper is to reveal the relationship between displacement and tilting angle of slope surface in shallow landslides. To investigate the relationship between the displacement and tilting angle, laboratory model tests with pre-defined slip surface were conducted under different triggering factors, such as tilting the slope model or applying artificial rainfall. In the model tests, tilt sensors with steel rods were installed in slope models to detect tilting behaviors of slopes, while the displacement of the slopes was approached by tracing the movement of marked points set on the tilt sensors. Additionally, field slope tests were also performed on natural slopes by applying artificial rainfall, in which the displacement and tilting angle of the slope surface were measured by extensometers and tilt sensors installed in the test slopes. In this study, the correlation between displacement and tilting angle of slope surface in shallow landslides was investigated and discussed under different testing conditions in model tests as well as in field tests.

Methodolody

Model tests

Two laboratory model tests were conducted. The slope model in these tests was built in a rectangular box, measuring 1165 mm (length) × 450 mm (width) × 380 mm (height), and composed of a base layer and a surface layer. The schematical illustration for the cross section of the slope models and arrangement of apparatuses employed in these tests are presented in Fig. 2.

To make the base layer, Silica Sand #7 (Fig. 3) with an initial water content about 10% was used, and compacted to a relative density larger than 90% by tamping. Then, the base layer was carved into a pre-designed shape, and the surface layer was built using the same sand with a relative density about 50%. The pre-designed shape consisted of two circular parts with the radius of 300 mm in the upper part and 800 mm in the lower part respectively. A polythene sheet was placed between the base layer and surface layer acting as the pre-defined slip surface of slope models due to the fact that the polythene can reduce friction and restrict water flow. After building the slope model, tilt sensors attached to long rods (T1 and T2) were installed with marked points set on the surface of these tilt sensors. In addition, an extra tilt sensor (T3) was fixed on the wooden box to measure the tilting angle of the box. In these model tests, a camera and a scale

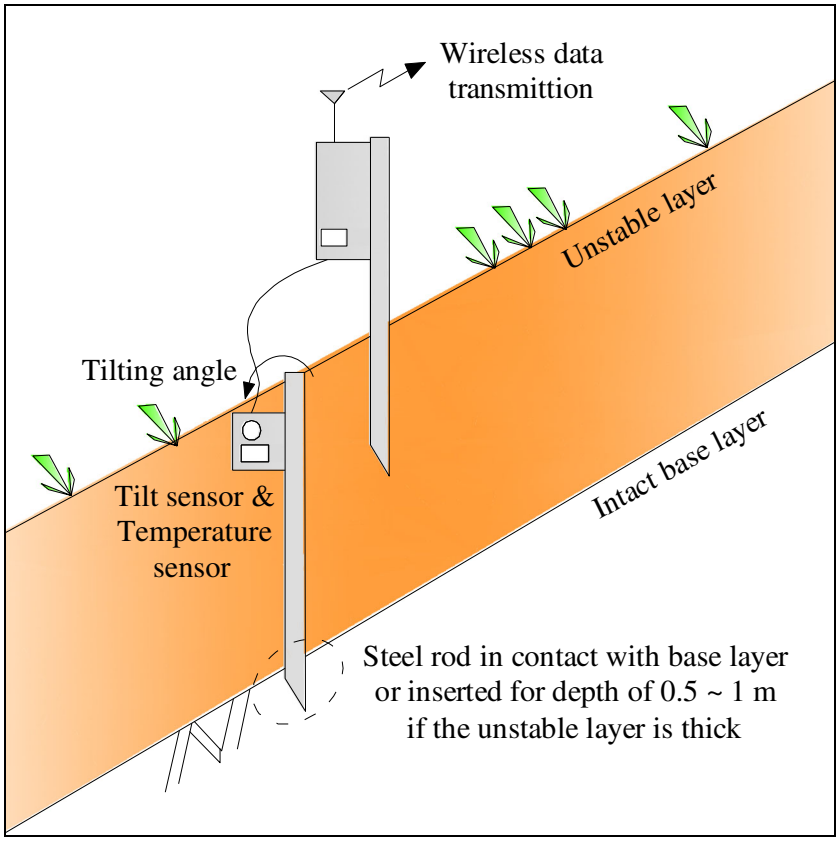

Fig. 1 The illustration of wireless unit with the tilt sensor and temperature sensor

were fixed over the slope model. The camera was used to record the surface movement of the marked points on the tilt sensors, while the scale was performed as a reference coordinate for image analysis. Since the movement of marked points was recorded by the camera using images, the location of the marked points in the images can be traced by using the reference coordinate system based on the scale. Then, the surface displacement of tilt sensors parallel to the slope surface can be calculated via the location change of the marked points. Additionally, the corresponding normal displacement of the tilt sensors to the slope surface was measured by using a vernier scale. The displacement of tilt sensors can be approached based on the sum of squares of the normal displacement and surface displacement. Considering that the tilt sensors were close to the slope surface, the displacement of tilt sensors is equivalent to the displacement of the slope surface. The slope failure in Model Test 1 was induced by tilting the box gradually using the mechanism chain as shown in Fig. 2a while the slope failure in Model Test 2 was triggered by applying periodical artificial rainfall as shown in Fig. 2b. In Model Test 2, the arrangement of experimental setup is the same as that in Model Test 1. After the installation of the instruments in the slope model of Model Test 2, the box was tilted to an target angle of 40°, and then artificial rainfall was applied. In these two laboratory model tests, the tilting angle of slope models was measured by tilt sensors, and the displacement was obtained by tracing the moving path of the marked points on tilt sensors.

Field tests

In addition, two field tests were also conducted on natural slopes on different sites. Field Test 1 was conducted on the Taziping landslide slope in Sichuan Province, China (Uchimura et al. 2015; Yang et al. 2017). This test site consists of loose gravel and sand, and the grain size distribution curve of the material on this site is presented in Fig. 4. The angle of the test slope is around 18°, and the lower end of the slope was excavated to a depth of 1.4 m with a slope angle of 60°. In this field test, the slope failure was induced by applying artificial rainfall using a rainfall simulator, and the displacement as well as the tilting angle of the failed part were measured by an extensometer E50 and a tilt sensor T50-2 installed in the region as shown in Fig. 5.

Field Test 2 was carried out in Baise city of Guangxi province where the weakly expansive clay is widely distributed. The soil particle size distribution in this region is presented in Fig. 6.

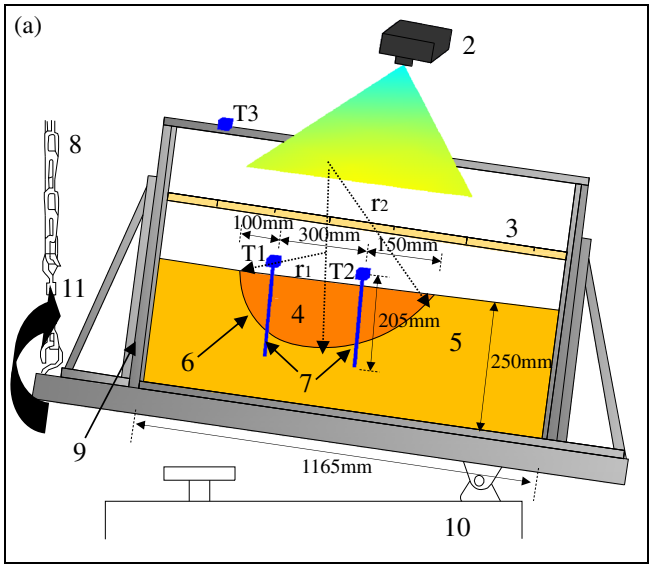

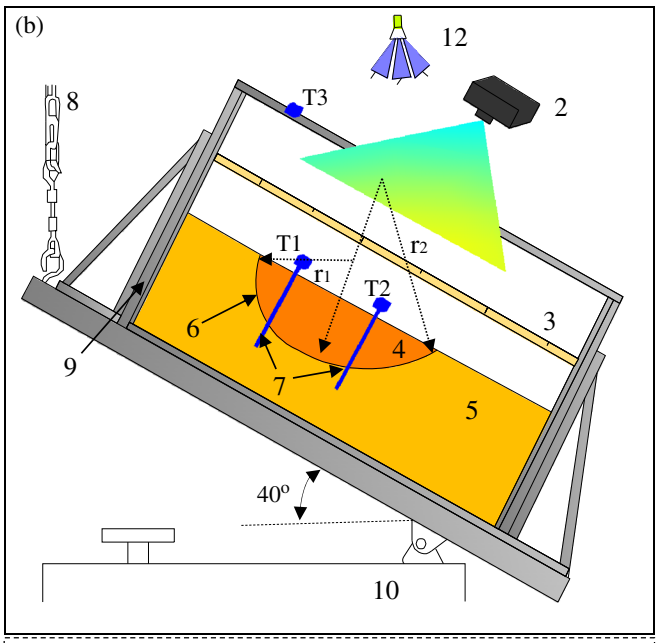

T1, T2 and T3-tilt sensors, 2-camera, 3-scale, 4-surface layer, 5-base layer, 6-pre-defined slip surface, 7-rods, 8-lifting mechanism, 9-lectangular box, 10-pivot support, 11-tilting the container, 12-artificial rainfall, r1, r2 -radius of slip surface, r1=300 mm and r2=800 mm

Fig. 2 Illustration for laboratory model tests. **a** The illustration of Model Test 1 in which the slope failure was induced by tilting the box. **b** The illustration of Model Test 2 in which the slope failure was induced by applying artificial rainfall

The slope angle of the test slope in this site is 43°, and a trench with a depth around 0.2 m was excavated at the toe of this slope. In this test, the slope failure was triggered by applying artificial rainfall with a constant rainfall intensity of 27 mm/h. The major deformation occurred in the middle part of this slope, which was recorded by the extensometer, E4 and the tilt sensor, T4. The illustration for the slope cross section and arrangement of sensors in this field test are presented in Fig. 7.

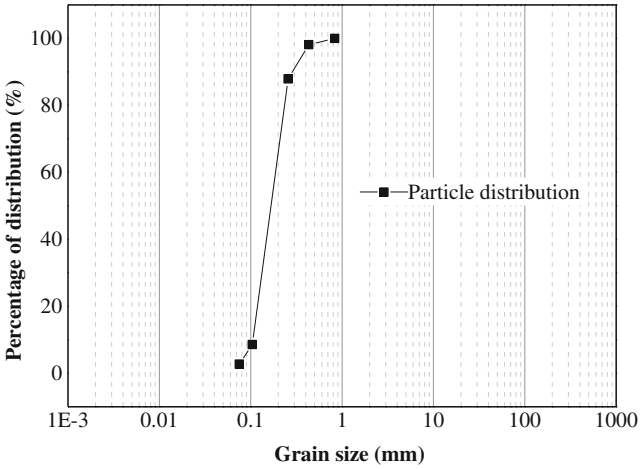

Fig. 3 Particle size distribution of Silica Sand #7

Result and discussion

Model tests

In Model Test 1, the slip surface consists of two circular parts with the radius of $r1 = 300$ mm in the upper part and $r2 = 800$ mm in the lower part respectively (Fig. 2). The slope failure in this test was induced by tilting the box gradually. The tilting history of the box was recorded by the tilt sensor T3 fixed on the box as shown in Fig. 2a, while the tilting behavior of the slope model was measured by the tilt sensor T1 and T2 installed in the slope. Figure 8a shows the time history of the tilting angle measured by T1, T2, and T3. The tilting angle of the slope induced by the slope deformation is equal to the different value between the tilting angle measured by the tilt sensors (T1 and T2) installed in the slope and that recorded by the tilt sensor (T3) fixed on the box. The tilting angle caused by slope deformation is presented in Fig. 8b. Figure 8c indicates the time history of slope displacement resulting from the surface

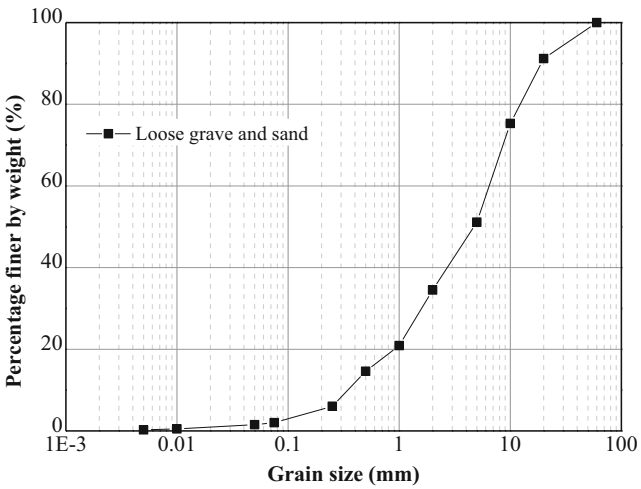

Fig. 4 Particle size distribution of the soil in Field Test 1

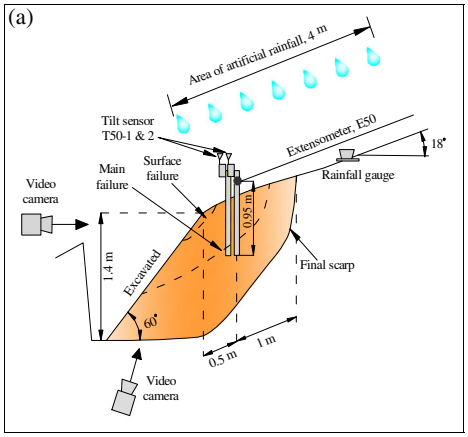

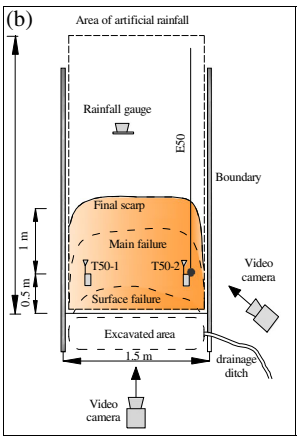

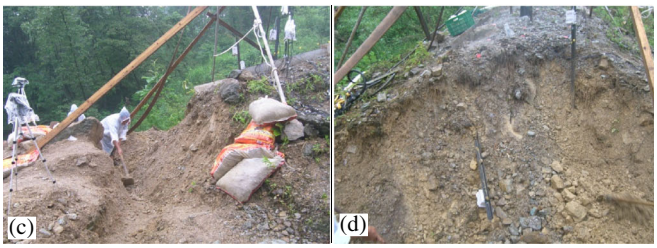

Fig. 5 The slope in Field Test 1. **a** The cross section of the slope and arrangement of sensors. **b** The front view of the slope and arrangement of sensors. **c** The image of the slope before slope failure. **d** The image of the slope after slope failure

displacement approached by image analyzing method and the normal displacement measured by a vernier scale. In Fig. 8d, the tilting angle is plotted against the displacement, and linear relationships between the tilting angle and displacement of the slope are indicated. The ratio of the fit line for T1 and T2 is around 211 mm/rad and 216 mm/rad respectively, coinciding with the length between the tip of rods and marked points on tilt sensors, 205 mm as shown in Fig. 2.

The slope failure of Model Test 2 was triggered by applying artificial periodical rainfall with a rainfall intensity 70 mm/h (Fig. 9a). Figure 9b and c show the time history of the tilting angle and displacement of the slope model, respectively. The relationship between the tilting angle and displacement of the slope surface is presented in Fig. 9d. The ratio of the fit line for T1 and T2 is around 231 mm/rad and 219 mm/rad, consistent

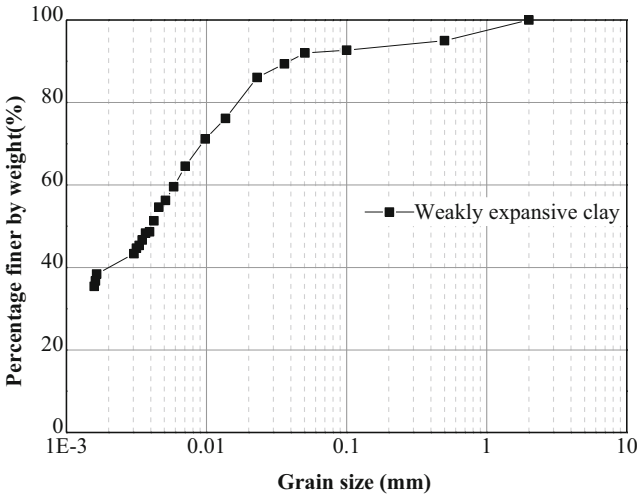

Fig. 6 Particle size distribution of the soil in Field Test 2

with the length between the marked points on the tilt sensors and the tip points of the rods, which was also 205 mm in this test. During the test, a small crack occurred near the location of T1 (Fig. 9e), accounting for the slight difference between the fitting ratio of T1 and T2.

Field tests

The results of Field Test 1 are shown in Fig. 10. The slope failure was induced by applying artificial rainfall and began at the bottom of the slope. The tilting behavior and movement of the slope surface were recorded by the tilt sensor T50-2 and extensometer E50. Figure 10a indicates the rainfall history, while the time history of tilting and displacement of this slope are presented in Fig. 10b and c respectively. As shown in Fig. 10b, c, the tilting angle was recorded by T50-2 every 2 min while the displacement was recorded every 1 min by E50. The average value of displacement in every 2 min is plotted against the tilting angle and indicated in Fig. 10d. A linear trend between the displacement and tilting angle is shown in Fig. 10d, and the fitting rate for the linear trend is 903.22 mm/rad, close to the length between the tip of the rod and the attached point of E50, 950 mm (Fig. 5a). The deviation from the linear trend as shown in Fig. 10d was caused by the tilting data fluctuation occurred around 35 h as shown in Fig. 10b.

The Field Test 2 was conducted on a nature slope consisting of weakly expansive clay, and the slope failure was induced by applying artificial rainfall with a constant intensity 27 mm/h. The major deformation occurred in the middle part of the slope where tilt sensor T4 and extensometer E4 were installed as shown in Fig. 7. The tilting angle and displacement of the failed part are presented in Fig. 11a and Fig. 11 b. Similarly, a linear relationship between the tilting angle and displacement is indicated in Fig. 11c, and the fitting rate for this linear relationship coincides with the actual length between the tip point of the rod and the attached point of extensometer E4, 300 mm.

Discussion

The slope failure in Model Test 1 was induced by tilting the box while the triggering factor of the slope failure in Model Test 2 was

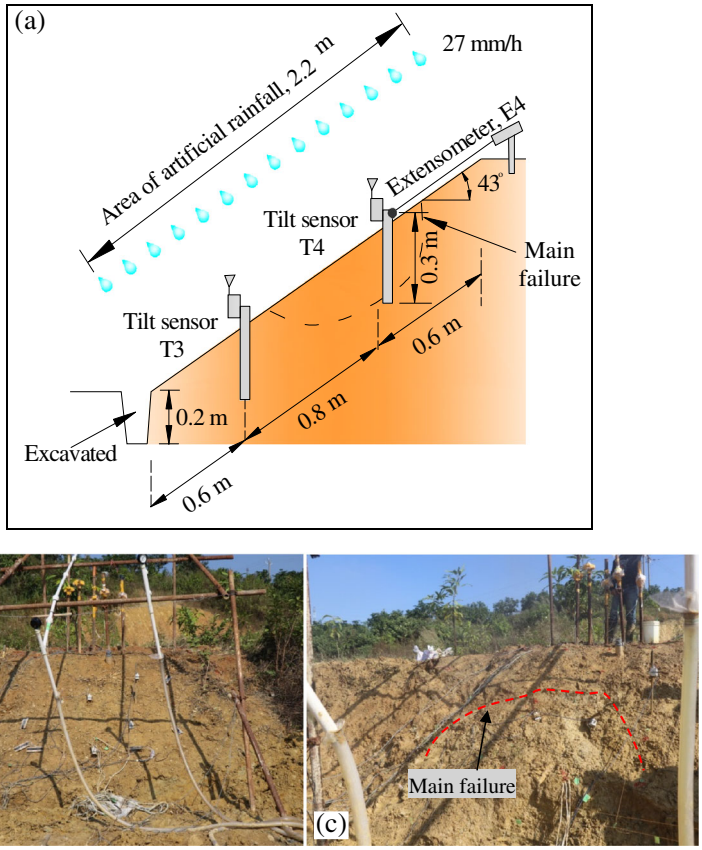

Fig. 7 The slope in Field Test 2. **a** The cross section of the slope and arrangement of sensors in Field Test 2. **b** Image of the slope before slope failure. **c** Image of the slope after slope failure

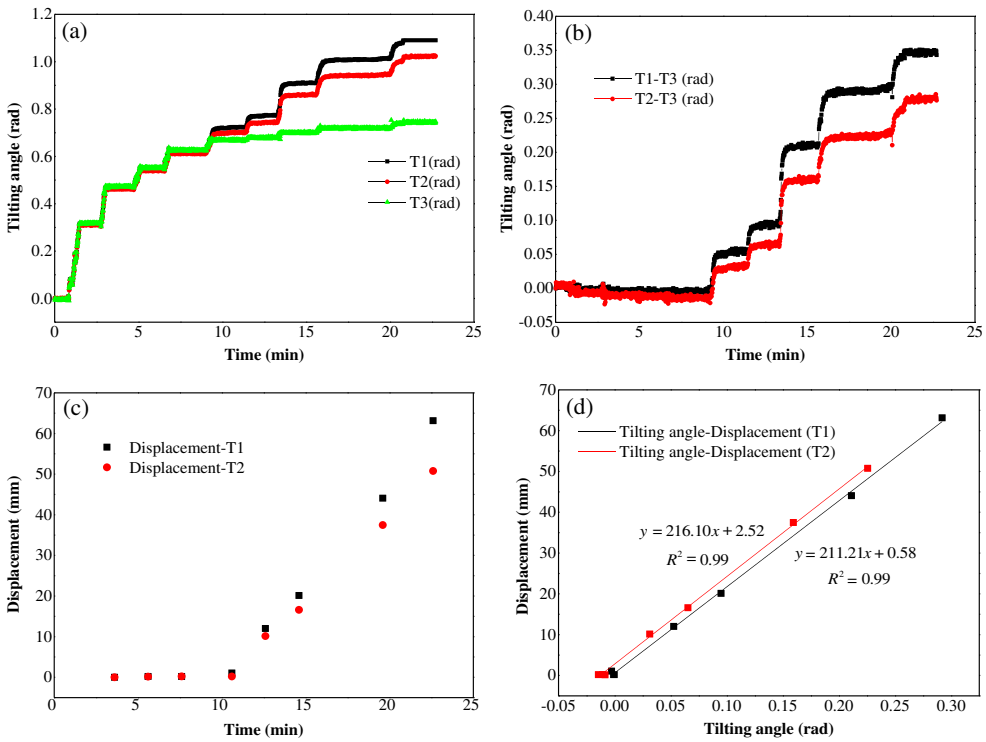

Fig. 8 The results in Model Test 1. **a** Tilting of the box and slope model against time. **b** Time history of tilting caused by slope deformation induced by tilting the box. **c** Displacement of slope surface against time. **d** Relationship between displacement and tilting angle of slope surface

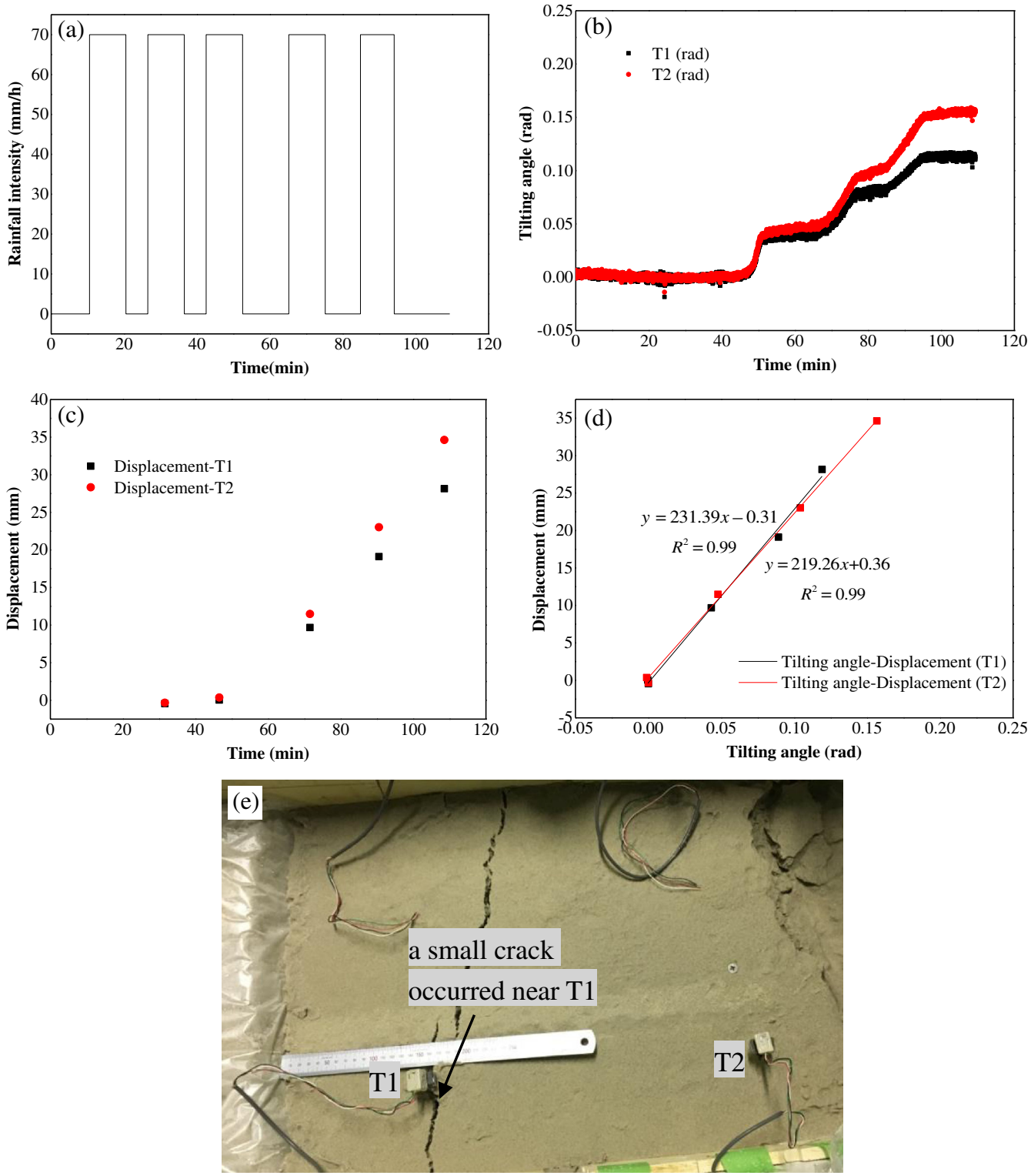

Fig. 9 The results in Model Test 2. **a** Time history of rainfall. **b** Time history of tilting caused by slope deformation induced by applying artificial rainfall. **c** Displacement of slope surface against time. **d** Relationship between displacement and tilting angle of slope surface. **e** A small crack occurred near T1

caused by applying artificial rainfall. Athough the triggering factors in these two model tests are different, the linear relationships between the tilting angle and displacement were observed. The consistent results imply that the linear relationship between the

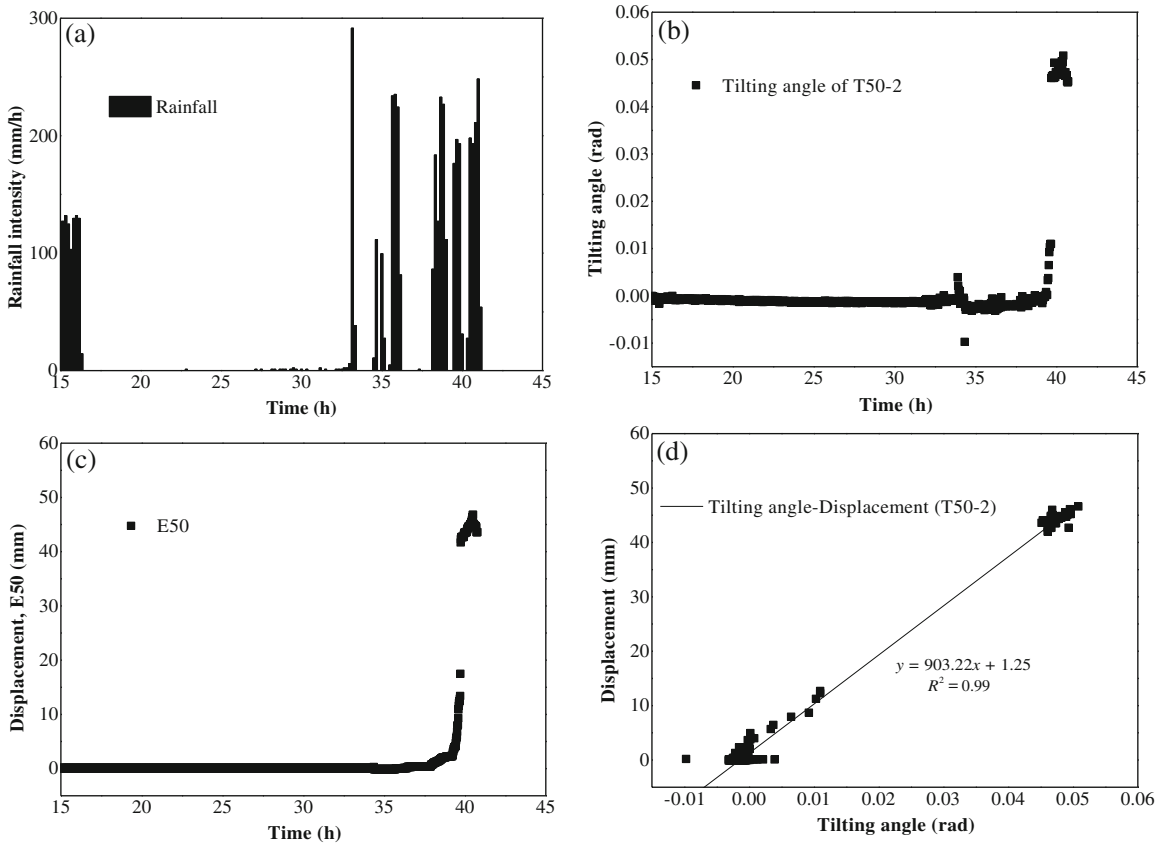

Fig. 10 The results in Field Test 1. **a** Time history of rainfall. **b** Time history of tilting measured by T50-2. **c** Time history of displacement of slope surface measured by extensometer E50. **d** Relationship between displacement and tilting angle of slope surface

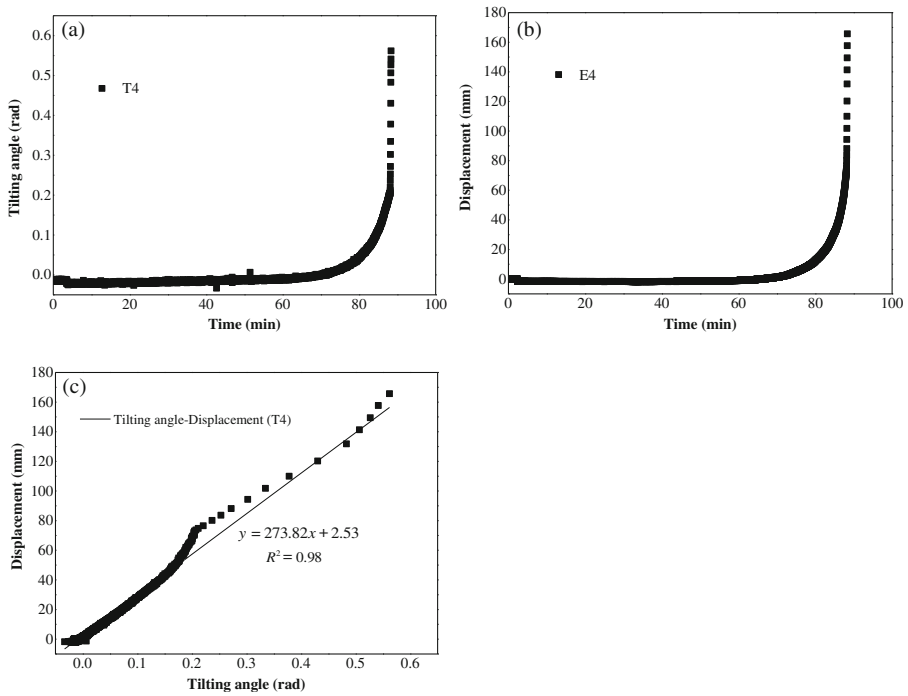

Fig. 11 The results in Field Test 2. **a** Time history of tilting measured by T4. **b** Time history of displacement of slope surface measured by extensometer E4. **c** Relationship between displacement and tilting angle of slope surface

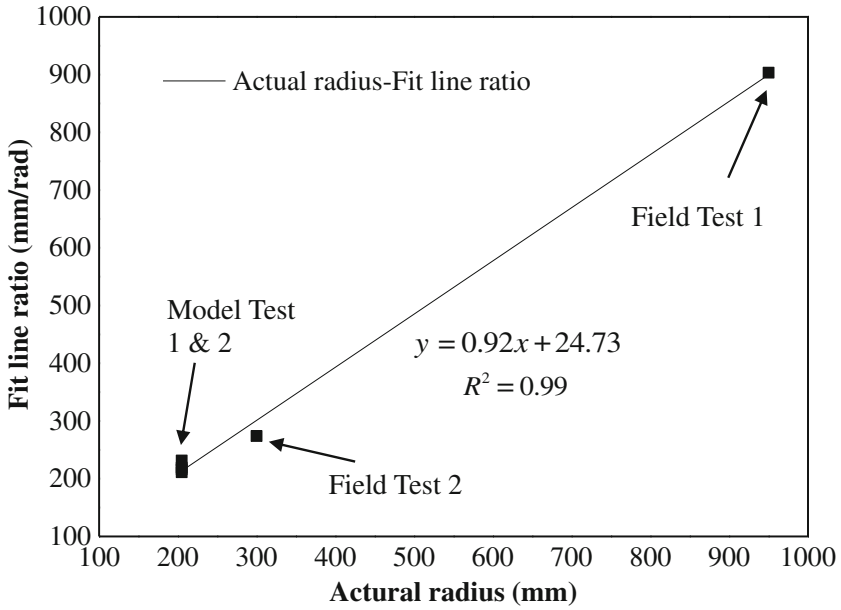

Fig. 12 The correlation between actual length and fitting rate of each sensor employed in the tests in this study

displacement and tilting angle is independent of the triggering factors of slope failure. In addition, two field tests were also carried out on nature slopes, and the slope failure in these tests was induced by applying artificial rainfall. The slope in Field Test 1 consists of loose gravel and sand, while the material of Field Test 2 is weakly expansive clay. Linear relationships between the displacement and tilting angle were also obtained in these two field tests in spite of that materials of these two slopes are different. Furthermore, the linear relationship is also independent of the slope size considering that consistent results were achieved in small scale model tests as well as in field tests.

The fit line ratio for the linear relationship between the displacement and tilting angle is plotted against the actual length for each sensor employed in the laboratory tests as well as field tests, and presented in Fig. 12. The figure shows that the value of actual length is close to the fit line ratio for the linear relationship between the displacement and tilting angle, and this result indicates that the tilt sensors with rods rotate against the tip points of the rods when slope was sliding, and the relationship between the displacement and tilting angle can be written as

$$\mathrm{ds} = r_i \cdot d\theta \tag{1}$$

where ds and $d\theta$ represent the displacement and tilting angle, respectively. r_i means the actual length between fixed point of rods and the position of sensors.

Conclusions

In this study, linear relationships between the displacement and tilting angle of slope surface were detected based on the results of laboratory tests and field tests, and this finding indicates that, similar as the displacement of slope surface, the tilting behavior of the slope surface can be treated as an indication of shallow landslides. The major findings of this study are presented as follows.

1. A linear relationship between the displacement and tilting angle of the slope surface was detected, and the equation for this linear relationship was also proposed as shown in Eq. (1).
2. The linear relationship is independent of triggering factors of slope failure. Although the triggering factors of slope failure in Model Test 1 and Model Test 2 are different, consistent linear relationships between displacement and tilting angle in these two tests could be obtained.
3. The linear relationship show no correlation with slope materials. Even though the materials of the slope in Field Test 1 and Field Test 2 are different, the linear relationship between the displacement and tilting angle was also indicated in these two tests.
4. The size effect on this linear relationship is negligible considering that consistent results were observed in model tests and field tests regardless of the different dimensions of the slopes.

Funding information

This research was supported by Chinese Scholarship Council (CSC, Grant No.201506370052) for PhD studies of the first author, and the Grants-in-Aid for Scientific Research of the Japan Society for the Promotion of Science (JSPS), Core-to-Core Program B (No. 16H04407).

References

Emanuele I, Giovanni G, Francesco M, Riccardo F, Nicola C (2012). Design and implementation of a landslide early warning system. Engineering Geology 147(148): 124–136

Fukuzono T (1985) A new method for predicting the failure time of a slope, Proc. IV, International Conference and Field Workshop on Landslides, Tokyo, pp 145-150

Iverson RM, Reid ME, Iverson NR, LaHusen RGLM, Mann JE, Brien DL (2000) Acute sensitivity of landslide rates to initial soil porosity. Science 290:513–516

Keefer DK, Wilson RC, Mark RK, Brabb EE, Brown WM, Ellen SD, Harp EL, Wieczorek GF, Alger CS, Zatkin RS (1987) Real-time landslide warning during heavy rainfall. Science 238:921–925
Petley D (2012) Global patterns of loss of life from landslides. Geology 40:927–930
Saito M (1987) On application of creep curves to forecast the time of slope failure. Journal of Japan Landslide Society 24:30-38
Towhata I, Uchimura T, Gallage CPK (2005) On early detection and warning against rainfall-induced landslide, Proc. of The First General Assembly and The Fourth Session of Board of Representatives of the International Consortium on Landslides (ICL). Springer, Washington, DC, pp 133–139
Uchimura T, Towhata I, Wang L, Seko I (2008) Simple and low-cost wireless monitoring units for slope failure. In: Proc. of the First World Landslide Forum, International Consortium on Landslides (ICL), Tokyo, pp 611–614
Uchimura T, Towhata I, Trinh TLA, Fukuda J, Carlos JBB, Wang L, Seko I, Uchida T, Matsuoka A, Ito Y, Onda Y, Iwagami S, Kim MS, Sakai N (2010) Simple monitoring method for precaution of landslides watching tilting and water contents on slopes surface. Landslides 7:351–357
Uchimura T, Towhata I, Wang L, Nishie S, Yamaguchi H, Seko I, Qiao J (2015) Precaution and early warning of surface failure of slopes by using tilt sensors. Soil Found 55(5):1086–1099
Yang ZJ, Qiao JP, Uchimura T, Wang L, Lei XQ, Huang D (2017) Unsaturated hydro-mechanical behaviour of rainfall-induced mass remobilization in post-earthquake landslides. Eng Geol 222(2017):102–110

J. Xie (✉) · T. Uchimura
Department of Civil and Environmental Engineering,
Saitama University,
255 Shimo-Okubo, Sakura-ku, Saitama, 338-8570, Japan
Email: jirenxie198911@csu.edu.cn

J. Xie
Department of Civil Engineering,
The University of Tokyo,
7-3-1, Hongo, Bunkyo-ku, Tokyo, 113-8656, Japan

P. Chen · C. Xie · Q. Shen
College of Civil Engineering and Architecture,
GuangXi University,
Nanning, 530004, China

J. Liu · Q. Shen
Department of Civil Engineering,
Hunan University of Technology,
Zhuzhou, 412000, Hunan, China